PERGAMON

Deep-Sea Research II 45 (1998) 2513–2530

DEEP-SEA RESEARCH
PART II

Hydroacoustic detection of volcanic activity on the Gorda Ridge, February–March 1996

Christopher G. Fox[a,*], Robert P. Dziak[b]

[a]NOAA, Pacific Marine Environmental Laboratory, Newport, OR 97365, USA
[b]NOAA/Oregon State University, Cooperative Institute for Marine Resource Studies, Newport, OR 97365, USA

Received 3 November 1997; accepted 14 January 1998

Abstract

Beginning at 0700 GMT on 28 February 1996, intense seismicity was detected in the northeast Pacific Ocean using the T-phase Monitoring System developed by NOAA/PMEL to access the U.S. Navy's SOund SUrveillance System (SOSUS) in the North Pacific. The event was preliminarily located on the northernmost segment of the Gorda Ridge near 42.67°N and 126.8°W, in the vicinity of the ridge segment high ("narrowgate"). The nature of the seismicity was similar to that observed in June 1993 at the CoAxial segment of the Juan de Fuca Ridge, which was later documented to be a lateral magma injection with subsequent eruption. Due to several gaps in the data, the detection information was not as comprehensive as during the CoAxial event, but an initial migration of epicenters from the narrowgate area down-rift is inferred based on arrival bearings from a single array; there is evidence for an additional diking event on the second and third day of activity. There is also indication of a concentration of epicenters located near 42.6°N, as occurred during the CoAxial episode at what was later determined to be an eruption site. Examination of T-wave rise times generally supports this interpretation. Based on the nature and duration of the activity, a response effort was initiated, which later confirmed hot-water plumes and fresh lava flows at the site. Based on both hydroacoustic information and field observations, it is proposed that the episode began with a lateral dike injection, possibly with eruptive activity in the summit region, followed by multiple magma pulses and eventual focusing of the seismic activity and extrusion near 42.6°N.
© 1999 Published by Elsevier Science Ltd. All rights reserved.

1. Introduction

Since June 1993, the National Oceanic and Atmospheric Administration's Pacific 2Marine Environmental Laboratory (NOAA/PMEL) has maintained a real-time

* Corresponding author.

0967-0645/99/$ – see front matter © 1999 Published by Elsevier Science Ltd. All rights reserved.
PII: S0967-0645(98)00081-2

acoustic monitoring system (T-phase Monitoring System) designed to detect volcanic seismicity along the seafloor spreading centers of the northeast Pacific Ocean. The system is capable of detecting water-borne seismic waves (T-waves) traveling in the oceanic sound channel. Acoustic signals are digitized from U.S. Navy underwater hydrophone arrays (the SOund SUrveillance System or SOSUS), and the digital data transferred in real time to NOAA/PMEL laboratories in Newport, Oregon. These signals are continuously analyzed and displayed, as described in Fox et al. (1995). The system is able to detect low-level seismicity down to magnitude 1.8 (Fox et al., 1994). The monitoring system depends on three hydrophone arrays located off the coasts of Oregon, Washington, and British Columbia, and covers the ridge system from the southern limit of the Gorda Ridge to the northern limit of the Explorer Ridge.

Shortly after installation in June 1993, the T-phase Monitoring System detected apparent volcanic seismicity along the Juan de Fuca Ridge, at a previously little-studied ridge segment later called the CoAxial segment (Fox et al., 1995). Detailed analysis of the hydroacoustic signals indicated a lateral dike injection, generally along pre-existing ridge crest fabric (Dziak et al., 1995), and changes in spectral characteristics of the recorded T-phases were interpreted to represent the gradual shoaling and surface eruption of this lateral dike down-rift (Schreiner et al., 1995). The hydroacoustic detections were later confirmed through extensive field studies by a multi-disciplinary team of NOAA and university investigators who diverted scheduled research expeditions to study this event (Fox, 1995, and related papers). Field observers documented evidence of seafloor eruptions and dike injection (Embley et al., 1995; Chadwick et al., 1995), large water-column hydrothermal plumes (Baker et al., 1995), and hydrothermal chemistry consistent with recent magmatic recharge in the sub seafloor (Massoth et al., 1995; Lupton et al., 1995). During the intervening years, extensive field work has continued at the site, although no other significant seismicity has been recorded. This was the first true detection and response effort for deep-sea volcanic activity.

This paper describes a similar seismic event recorded in February–March 1996 emanating from the northern Gorda Ridge. Due to numerous difficulties related to severe weather in the Pacific Northwest, the acoustic record for the Gorda Ridge episode discussed in this paper was not as complete as for the CoAxial segment event. The severe winter weather also had a large impact on the availability and operability of research vessels for response. This paper presents our best interpretation of this incomplete acoustic record and compares the observations to what was learned from the CoAxial event and the current understanding of the crustal accretion process. There are significant differences in the nature of the two episodes.

2. Event detection

Beginning at 0700 GMT on 28 February 1996, intense seismicity similar to that observed from the CoAxial segment in 1993 was detected by the T-phase Monitoring System (Fig. 1). The general nature of the seismicity was consistent with magmatic processes: low-level earthquakes in rapid succession lasting for many hours. As was

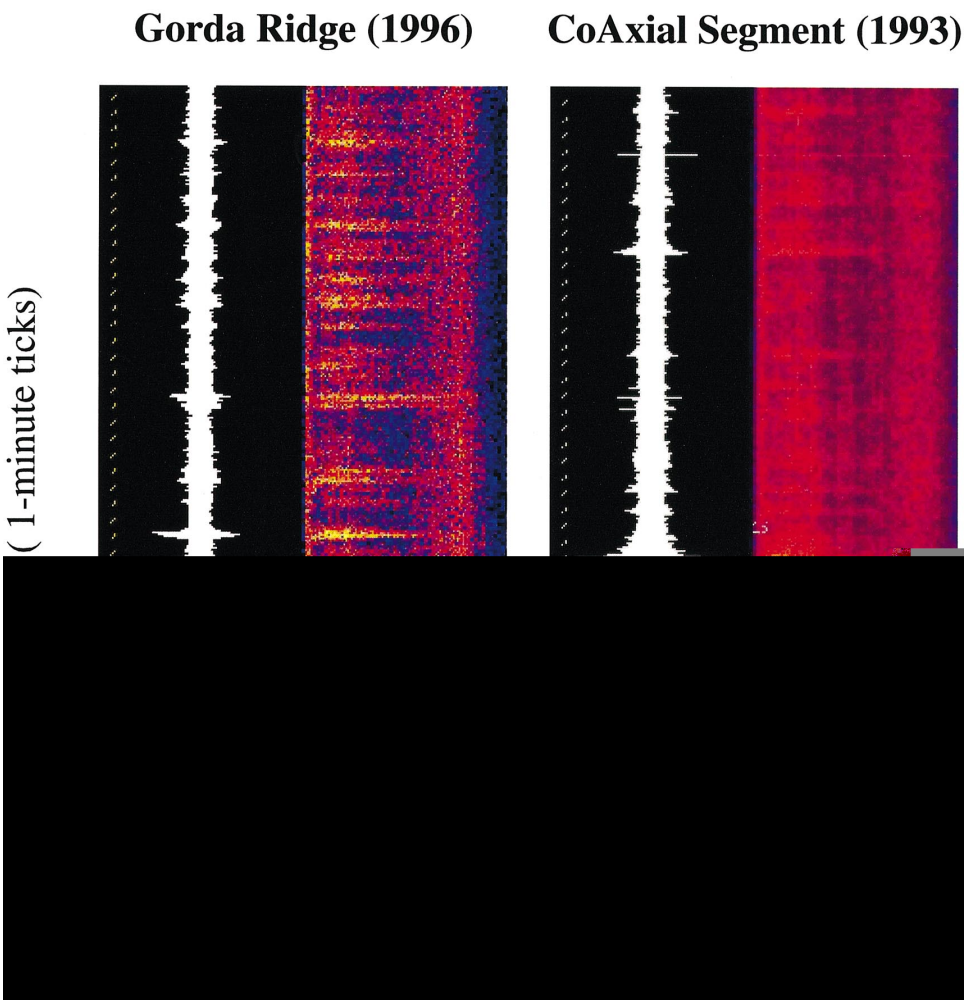

Fig. 1. Comparison of spectrograms from the 1996 volcanic event at Gorda Ridge (left) and the 1993 event at the CoAxial segment of the Juan de Fuca Ridge (right). The horizontal axes display beam-former electrical amplitude ($\pm$ 5 V) and frequency range [0–75 Hz (left), 0–50 Hz (right)]. The vertical axes display time with each tick representing 1-min interval. Both events show the character of volcanic seismicity recorded hydroacoustically: rapidly repeating small earthquakes centered in the 5–15 Hz frequency band.

the case during the 1993 CoAxial segment activity, there was no measurable seismicity recorded on the land-based seismic networks in the Pacific Northwest (John Nabelek, Steve Malone, personal communications). During the initial 42 h of activity, no position for the event could be derived since two of the three SOSUS arrays required for accurate epicenter location were inoperable due to a large North Pacific storm that disabled the shore station at Pacific Beach, Washington. The array closest to the site of activity was available and provided excellent recordings of the nature of the activity and a general sense of the location on the Gorda Ridge.

After all three SOSUS arrays were restored at 0100 GMT on 1 March 1996, an initial position was derived for the site of activity at 42.67°N, 126.8°W. This preliminary position ultimately proved to be within 2 km of the first detected hydrothermal plume (see Baker et al., 1998) and within 1 km of the location of eruptive lavas (see Chadwick et al., 1998). The epicenter location lies near the western boundary fault of the "narrowgate", or ridge segment high axial valley, of the northernmost segment of the Gorda Ridge, or North Gorda Ridge (Fig. 2). All subsequent epicenters fell within this segment (see below). After 35 h with all three arrays operational, the hydrophone array closest to the event was lost at 1200 GMT on 2 March 1996 to another storm and was restored by Navy personnel at 2300 GMT on 5 March 1997. During that 83-h hiatus, the detection threshold was higher, and accurate epicenter locations could not be derived (see event histogram in Fig. 3). All arrays were operational for the remainder of the episode.

The overall level and duration of the events were similar to those observed at CoAxial segment (Fig. 3), although the total number of detected events was somewhat higher for the Gorda Ridge event (4093 detections) than the CoAxial segment event (2984 detections). This difference in the number of events detected may be due to differences in propagation, ambient noise, or proximity and sensitivity of the nearest sensor. Hooft and Detrick (1995) have inferred a thinner crust, but thicker brittle layer, for the Gorda Ridge relative to the Juan de Fuca Ridge, which may allow generally larger magnitude earthquakes and therefore more detections. The duration of both the Gorda Ridge and CoAxial segment episodes was just over three weeks. Of course, smaller events beneath the detection threshold of SOSUS may have continued for several weeks after the end of SOSUS-detected activity. If the three-week duration of both episodes is typical of seafloor spreading events, this is a reasonable length of time to mount a field expedition with proper preliminary planning. No subsequent volcanic seismicity has been detected at the site as of this writing (March 1998).

3. Distribution and nature of seismic activity

The distribution of epicenters derived from acoustic monitoring are largely confined to the southern flank of the northernmost segment of the Gorda Ridge (Fig. 2). The predominant majority of epicenters lie between the segment bathymetric high ("narrowgate") located near latitude 42.75°N, and the southern limit of the segment at 42.4°N, a total distance of approximately 40 km. Several epicenters locate on the northern flank of the segment, but these are not necessarily directly involved in the

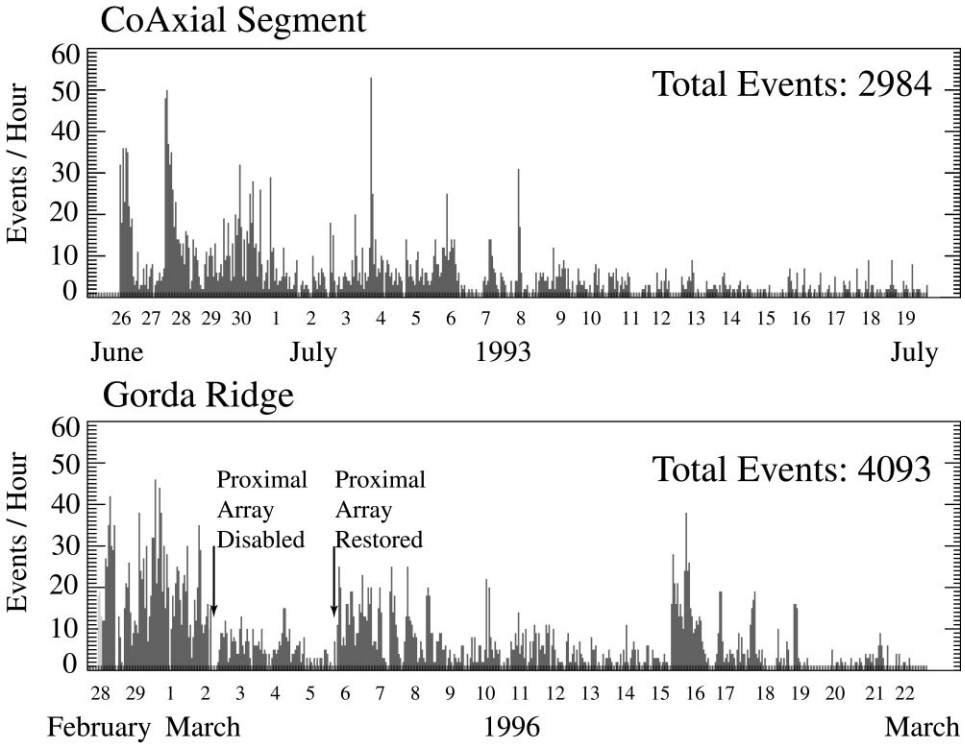

Fig. 3. Comparative histograms for the 1993 CoAxial segment volcanic event (above) and the 1996 Gorda Ridge event (below). Each bar represents the number of earthquakes recorded per hour from the respective sites. Both sequences last over three weeks and show nearly continuous activity with considerable variability on an hourly basis over the period. Data from the SOSUS array nearest to the Gorda Ridge event was unavailable during 2–5 March 1996 resulting in an artificially reduced number of recorded earthquakes. The total number of identified events for the CoAxial episode is 2984 versus 4093 for the Gorda Ridge episode.

volcanic episode. The background seismicity level for this segment averages several events per week, and therefore these earthquakes, along with some subset of events on the southern flank, may represent normal fault plane movements on the bounding faults with no direct relation to seismicity from the magma system.

The initial epicenter location provided to the field parties was at 42.67°N, 126.8°W, south of the narrowgate on the western side of the rift valley. The main seismic swarm that followed also appeared to be offset slightly to the western boundary of the rift valley in the northern areas, and field investigators were directed to that target area. In the downrift region, the epicenters appeared to be centered in the rift valley. No activity was observed in the adjacent segment to the south (below 42.4°N).

A more detailed look at the time distribution of the activity reveals some interesting patterns (Fig. 4). In the case of the CoAxial segment episode in 1993, the distribution

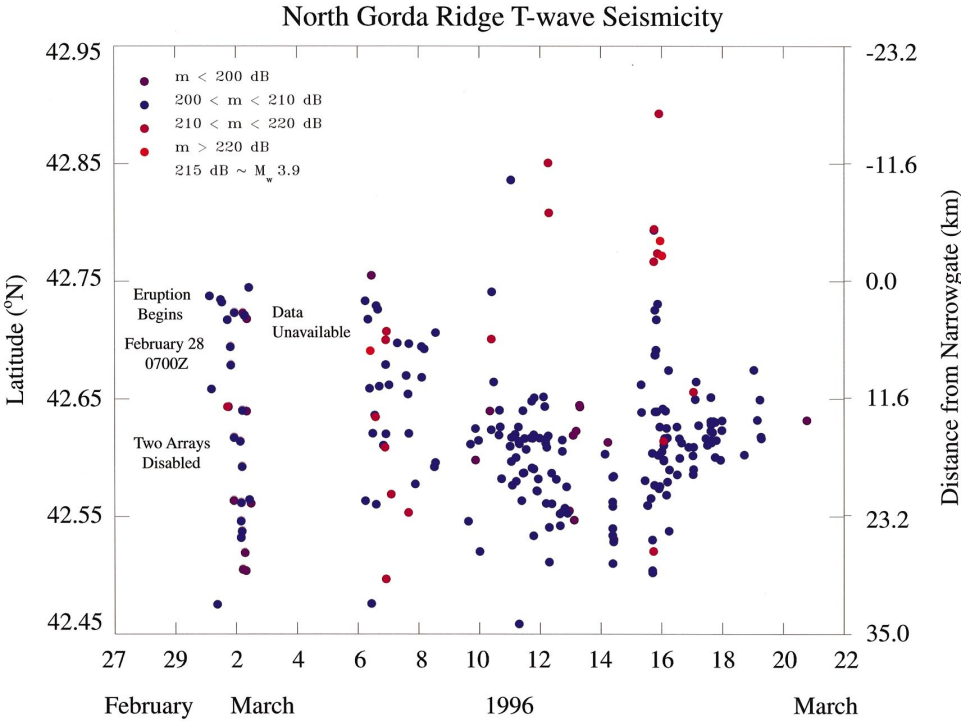

Fig. 4. The distribution of seismic activity through time is shown as epicenter latitude versus time. Unlike the 1993 CoAxial segment episode which showed a simple down-rift migration followed by eruption, this sequence is a complicated series of lateral migrations and focused events. Time periods of missing data are also shown. Estimated earthquake magnitudes are shown in color.

of epicenters clearly showed an initial migration of activity downrift over the first two days of activity (Dziak et al., 1995). Following this 60-km migration, the activity concentrated at a single location that later was observed to be the site of lava extrusion on the seafloor. The initial seismic migration at CoAxial segment actually progresses 10–12 km beyond the eventual eruption site (Dziak et al., 1995, Fig. 3).

The time-space distribution of the seismicity during the Gorda Ridge episode is significantly different from the simple down-rift migration followed by eruption sequence observed at CoAxial segment. Fig. 4 shows that rather than a simple downrift migration with focusing at a single site, the Gorda Ridge episode consists of multiple seismic sequences spanning large portions of the southern flank of the segment. In order to evaluate whether these sequences represent down-rift migrations, possibly due to multiple episodes of magma injection, selected episodes were studied in isolation. The change in latitude through time for individual episodes will be presented in the following section.

Schreiner et al. (1995) developed a protocol for relating T-wave arrival structure to hypocentral depth that relies on the rise time of an individual arrival; that is, the time interval between the initial appearance of the T-phase energy above ambient noise to the time of peak energy. During the CoAxial segment eruption in 1993, the T-wave rise times ranged from 12 s to less than one second with a progressive decrease of rise times throughout the episode. The activity occurred in discrete swarms, with early swarms ranging from 12–4 s rise time duration, while later swarms reduced to 4–0.5 s duration. This change in rise time was interpreted to reflect the shoaling and eventual eruption of the dike as it propagated to the north. Shallower focal depths result in more areally concentrated motion on the overlying seafloor and therefore shorter rise times and higher frequency content for T-waves coupled into the oceanic sound channel. The very short rise times (< 2 s) were interpreted to represent actual eruption on the seafloor. Observing both the migration of epicenters down-rift and the shoaling of focal depths (based on shorter rise times), magma dike injection can be inferred. Least-squares estimation of the migration speed can be compared to other volcanic sequences. Concentration of activity at a given latitude combined with short T-wave rise times might indicate actual seafloor extrusion.

4. Evidence for multiple magma injections

Using the methods described above, individual seismic sequences can be examined to infer magma injection and extrusion. For convenience, these sequences will be numbered. Of particular interest is the initiation of seismicity, which in the case of the CoAxial segment produced a migration of approximately 60 km in 36 h. Unfortunately in the case of the Gorda Ridge event, only a single SOSUS array was available during the initiation of the event and epicenter locations cannot be directly calculated. Evidence for an initial, significant lateral dike propagation can be derived from the arrival bearings at the single array. The NOAA/PMEL T-phase Monitoring System collects signals from two individual hydrophone elements located hundreds of meters apart within each SOSUS array. Arrival bearings for incoming T-waves are routinely

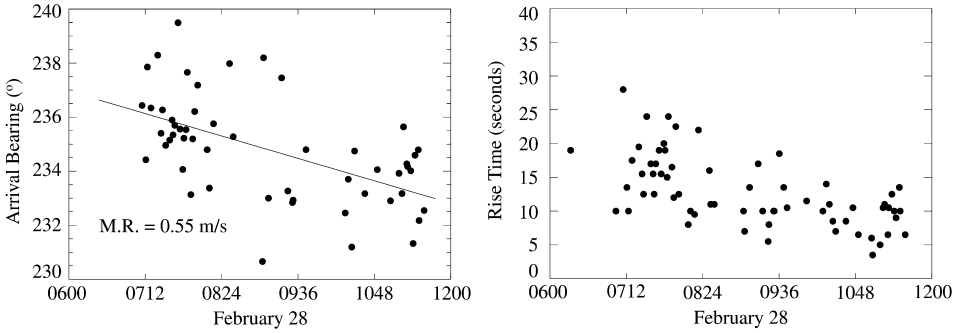

Fig. 5. The initial seismic swarm (Event 1) is shown in the top diagram as arrival bearing versus time (GMT). Since only one SOSUS array was available during the recording period, the southward migration of the seismicity can only be observed as a change in arrival bearing through time. The rise times of each event are shown below. The steady decrease in rise time through time is interpreted to represent the shoaling of the magma dike beneath the seafloor. Based on the general geometry and range to the site, a migration rate of 0.55 m/s was calculated.

calculated through an examination of the cross-spectral energy in a selected frequency band (5–30 Hz) that contains the majority of the T-wave energy. This information is normally used for event association only, since it does not yield accurate positions; but a systematic change in arrival bearing from the initial earthquake sequence would indicate lateral migration of the T-wave epicenters.

For the relative geometry of the Coos Bay SOSUS array and the northern Gorda Ridge, a southward propagation of T-wave epicenters should appear as southwest bearings with decreasing arrival bearings. Fig. 5A shows the arrival bearings through time for the initial seismic swarm (Event 1) on the Gorda Ridge. The arrival bearings can be seen to decrease from 240° to 232° over a 5-h period ending midday on 28 February 1996. An attempt was made to relate these bearings to ridge-crest locations by comparing the bearings of later, well-located epicenters, but the results were not reasonable indicating some bias in the bearing information. By applying the average range from the listening array to the ridge crest and performing a linear least-squares fit of the data, a migration rate of approximately 0.55 m/s is derived for this initial event. This is twice the rate calculated for the initial injection event at CoAxial segment (Dziak et al., 1995). Fig. 5B shows the corresponding T-wave rise times for the Event 1 swarm. The trend toward shorter rise times as the sequence progresses is evident and implies a shoaling of the corresponding hypocenters. The shortest rise times of approximately five seconds are substantially longer than those observed at CoAxial segment (Schreiner et al., 1995). This may imply that there was no subsequent seafloor eruption, but may also be due to the generally rougher seafloor of the Gorda Ridge providing a more diffusive acoustic radiator.

Following this initial T-wave swarm, a second significant swarm (Event 2) was observed beginning midday on 1 March 1996 and lasting approximately 24 h. In this case, all three SOSUS arrays were available and accurate epicenter locations were calculated. A comparison of latitude with time (Fig. 6A) indicates another southward

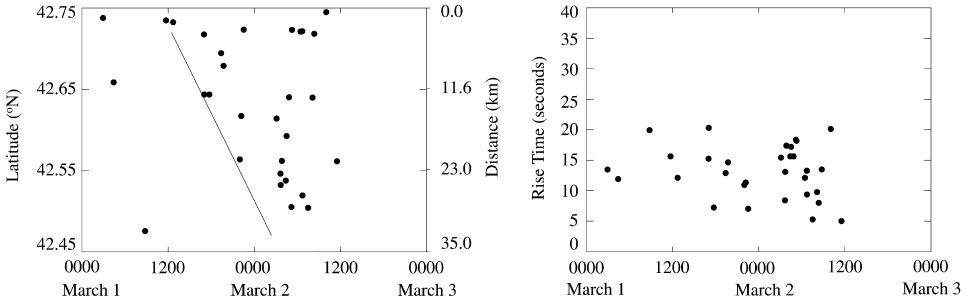

Fig. 6. The propagation of seismicity during Event 2 on 1–3 March 1996 is shown in the top diagram as latitude versus time. The rate of propagation of the leading edge (illustrated by a line) is comparable to the 0.55 m/s rate estimated for Event 1. No progressive change in rise times is observed (bottom), but the derived values are similar to the shorter rise times recorded near the end of Event 1, indicating a relatively shallow focal depth.

migration of epicenter, but in this case seismicity continues in the up-rift region as the southern limit of the swarm extends down rift. A direct least-squares fit is not appropriate in this case, but the migration rate of 0.55 m/s estimated for Event 1 provides a reasonable limit for this event as well. The rise times for Event 2 (Fig. 6B) do not indicate any progressive change in hypocenter depth through time, but all of the rise times are comparable to the later, shoaler stages of Event 1. Again, no postulation on the presence or absence of seafloor extrusion can be made from these data.

Following Event 2, the proximal SOSUS array at Coos Bay was lost for more than three days and no interpretable locations or bearing could be derived. After restoration of the array on 6 March 1996, the pattern of seismicity with latitude appears quite complex, with epicenters throughout the segment (Fig. 4). This pattern reflects the presence of after shocks to previous events that may be mixed with additional magma injection events. One interesting sequence occurs late on 15 March 1996 and includes the entire segment from near the Blanco Fracture Zone intersection to the southern limit of the segment (Event 3). There is no indication of lateral migration in this sequence, and it contains some of the largest magnitude events in the entire data set. This broad event is interpreted to represent extensional movement on the bounding faults of the segment and is not necessarily involved with the magmatic activity occurring on the southern portion of the segment, although one could argue that removal of underlying magma may have triggered the event. One large event from this sequence (magnitude $M_w = 3.9$), located at 42.9°N and 126.675°W, was recorded by land seismic stations and shown to be a normal fault with N26°E strike and a dip of 50° (Jochen Braunmiller, Oregon State University, personal communication), which is consistent with extension along the bounding faults.

During the 1993 CoAxial segment episode, the seismicity eventually concentrated at a single location that was later confirmed to be the site of seafloor lava extrusion (Fox, 1995). A similar concentration of epicenters (Event 4) appears to begin on 10

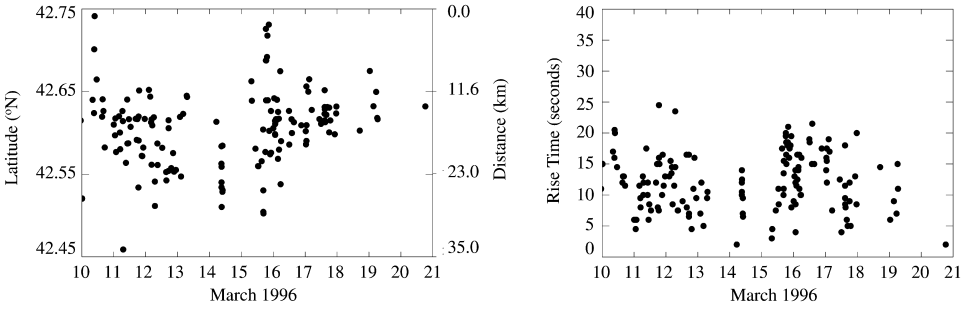

Fig. 7. Region of focused seismicity near 42.62°N beginning on 10 March 1996 and lasting until 21 March 1996. This seismicity is interpreted to represent an eruptive phase of the sequence, and shows no systematic migration (shown above). Rise times (shown below) are among the shortest in the entire data set, consistent with this interpretation.

March 1996 near latitude 42.6°N as shown in Fig. 7A. The same sequence can be seen as a cluster of epicenters located near 42.62°N and 126.8°W in Fig. 2. There is no evidence of epicenter migration through time. The focused events are mixed with other sequences from normal faulting or magma injections. The rise times for this event, although longer than those recorded from CoAxial segment, are the shortest of the Gorda Ridge episode, with many measured at less than five seconds. This sequence is the most compelling evidence for seafloor extrusion within the data set.

5. Relationship to field observations

Fig. 8 summarizes the interpretation of the available hydroacoustic data presented in the previous section. A lateral dike injection is inferred on 28 February 1996 (Event 1), with renewed magmatic intrusions occurring on 1–2 March 1996 (Event 2) and in the later stages of the episode. The long sequence on 15 March 1996 (Event 3) is interpreted to represent extension on the bounding faults, with a possible extrusive episode (Event 4) occurring on 10–21 March 1996.

Shortly after the onset of activity, NOAA/PMEL began planning a field response effort. Due to the time of year, there were no research ships working in the area and a limited number of vessels available in nearby ports. The NOAA Ship *McArthur*, a mid-sized research vessel normally used for shallow water research, was between cruises in Seattle and was made available for a response effort. The vessel had limited over-the-side capabilities, but did carry a 3100 m conducting cable and CTD winch capable of collecting vertical hydrographic casts to 2900 m. Dr. Ed Baker of PMEL led the expedition (GREAT 1) to attempt to identify, map, and sample hydrothermal event plumes over the site.

McArthur arrived at the study area on 8 March 1996 and began to collect hydrographic casts, beginning at latitude 42.436°N and proceeding north at 2 nm intervals (Baker, 1998). Hydrothermal event plumes were first detected at 42.602°N,

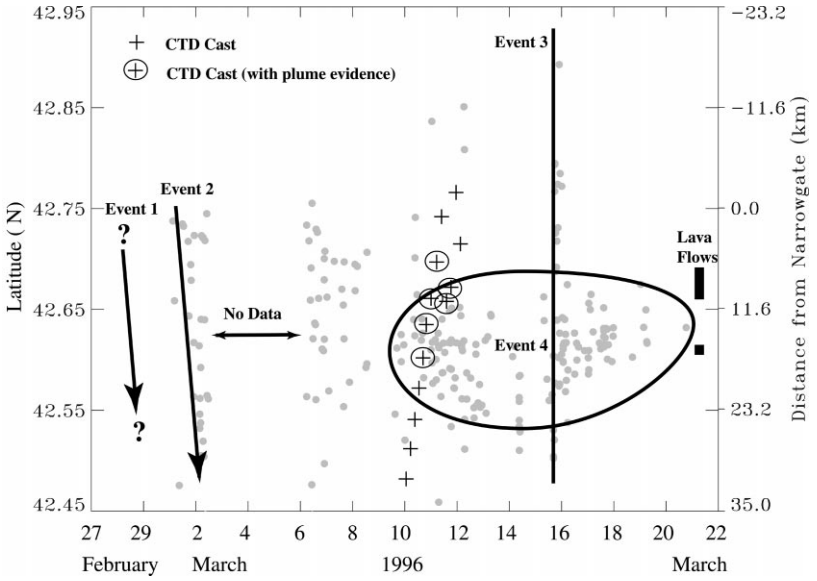

Fig. 8. Interpreted summary of the seismic sequence observed from the 1996 Gorda Ridge episode. At least two initial migrations (Events 1 and 2), likely due to lateral magma intrusions, are followed by a data gap and complex seismicity which may contain additional migration sequences. Event 3 is a large time-synchronous sequence representing horizontal extension on the bounding faults, which may or may not be related to the magmatic activity. From 10–21 March 1996, seismicity focuses at 42.62°N, in what may represent an eruptive sequence. CTD hydrocasts (shown as crosses) are plotted with circled crosses identifying hydrocasts showing evidence of hydrothermal event plumes (see Baker et al., 1998). These latter casts correspond well to the inferred time and location of possible magma extrusion. The latitude range of observed (upper) and inferred (lower) lava flows, based on bathymetric differences and camera images (Chadwick et al., 1998), are shown at the right, again supporting the interpretation of lava extrusion during Event 4.

126.825°W on 10 March 1996. Fig. 8 shows the location of the vertical casts and indicates those that showed hydrothermal plume anomalies. The time of the plume discovery was within 12 h of the inferred onset of the focused seismicity of Event 4 and was clearly within the latitude range of the seismic activity. Subsequent casts confirm a plume that generally occured in the inferred latitude range of the activity, although extending somewhat north of the seismicity (Fig. 8; Baker, 1998). This offset could be due to either error in the epicenter locations or drift of the plume to the north. Later plume studies are discussed by Baker (1998), Cowen et al. (1998), Feely et al. (1998), and Massoth et al. (1998).

Seafloor geological investigations were conducted in April from the Oregon State University R/V *Wecoma* using a deep-towed camera system, and a fresh lava flow was imaged near 42.675°N, 126.783°W (Chadwick et al., 1998). Subsequently, a multibeam bathymetric survey was collected over the site from the NOAA Ship *Discoverer* in June, 1996, and the result compared to pre-existing surveys collected in 1980–81 from

NOAA ships. The quantitative comparison of these two bathymetric surveys, using a method developed by Fox et al. (1992), indicates both the fresh lava flow imaged by camera and an additional bathymetric anomaly that may represent a smaller lava flow located near 42.610°N, 126.820°W (Chadwick et al., 1998). These two flows (one confirmed and one inferred) indicated (Fig. 8) fall generally in the latitude range of the seismically focused Event 4, with an offset to the north similar to the hydrothermal plume data. Both flows could have formed simultaneously during Event 4, with the offset representing a southward bias in earthquake epicenter location for the swarm. Another possibility is that the northern lava flow was formed during an earlier episode centered in that latitude range, during the 83-h period that data from the closest SOSUS array was unavailable, while the southern flow was formed during Event 4. There are no other data to support or refute this possibility. The smaller flow to the south has not been confirmed by deep-sea camera, but does appear as a likely feature on high-resolution sidescan. The rough terrain of the Gorda Ridge and poor navigation of the earlier surveys make the bathymetric comparison technique less reliable for this area (Chadwick et al., 1998).

5.1. Estimating extension from T-wave seismicity

The total horizontal extension occurring across a mid-ocean ridge during a seismic swarm can be estimated by approximating the integrated seismic moment of the component earthquakes within the swarm (Solomon et al., 1988). This estimate is further complicated for hydroacoustically recorded T-waves, since the seismic to hydroacoustic energy conversion process through the seafloor–ocean interface is poorly understood. Dziak et al. (1997) present an empirical method for estimating seismic moment from the predicted acoustic source level at the epicenter of oceanic earthquakes. Producing source level estimates involves integrating the T-wave signal over its optimum S/N frequency band (5–30 Hz), adjusting for the acoustic transmission loss along the propagation path from source to receiver (typically 10–20 dB), and removing instrument gain which results in an estimate of the acoustic pressure (in dB) the earthquake projects into the water column. Averaging the source level estimates at all hydrophones recording the earthquake provides an average acoustic energy value at the oceanic epicenter that can then be compared to seismic magnitude and moment. Following this approach, Dziak et al. (1997) showed that acoustic source level scaled linearly with the log of seismic moment for 14 earthquakes ($2.8 \leqslant M_L \leqslant 5.3$) from the April 1992 Cape Mendocino earthquake sequence, and that this relation can be reliably fit with a simple linear regression model.

Since 1992, routine estimates of the seismic moments of northeast Pacific Ocean earthquakes have been available from Oregon State University's seismology laboratory (John Nabelek, pers. comm.). During this time period, twelve earthquakes ($M_w > 3.5$) have occurred along the northern Gorda Ridge segment that were recorded by both seismograph and hydrophone arrays. This allows the development of a relationship between the seismic moment release and T-wave source level of northern Gorda Ridge earthquakes. Fig. 9 and Eq. (1) show the scaling relationship of acoustic source power level to seismic moment derived from the twelve northern

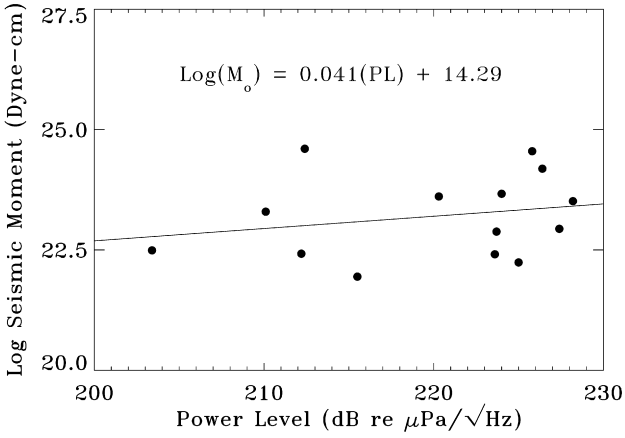

Fig. 9. Scaling relationship of acoustic source power level to seismic moment of twelve earthquakes ($M_w > 3.5$) that occurred along the northern Gorda Ridge from August 1992 through December 1996. The regression line and equation derived from the data are shown. The errors in slope and Y-intercept are ± 0.01 and ± 1.8, respectively. The regression fit has an R^2 of 0.72. This linear relationship between hydrophone recorded acoustic power and log seismic energy allows for estimates of the seismic moment release of northern Gorda Ridge earthquakes based on their hydrophone records.

Gorda Ridge earthquakes using the method of Dziak et al. (1997),

$$\mathrm{Log}(M_0) = 0.041(SL) + 14.29, \tag{1}$$

where M_0 is seismic moment in units of dyne-cms and SL is T-wave source level in power units of decibels relative to micro-Pascals (pressure) at 1 m from the source. Coincident data from other areas of the NE Pacific Ocean were not used to supplement the northern Gorda Ridge regression fit because acoustic and seismic parameter scaling relations have been shown to have significant geographic variation (Dziak et al., 1996) and might introduce errors of nonstationarity into the regression model. The relationship presented in Eq. (1) was applied to all recorded T-wave earthquakes from the 1996 eruptive event on the northern Gorda Ridge and the total seismic moment release is estimated at 1.3×10^{25} dyne cm. This represents a minimum estimate since it does not include earthquakes that occurred during recording gaps and small events beneath the hydrophone detection threshold ($m_b \sim 1.8$; Fox et al., 1994).

Applying the simple model of lithospheric extension along a ridge axis median valley floor presented by Solomon et al. (1988) allows for an estimate of the horizontal extension along the northern Gorda Ridge due to the 1996 swarm event. Solomon et al. (1988) developed this generalized model for Mid-Atlantic Ridge (MAR) segments and assumed that extension occurs predominantly by normal faulting of the brittle lithosphere. This is admittedly not the case for the northern Gorda Ridge episode since magma dike injection is involved and a significant amount of plate separation likely occurs from aseismic extension due to injection of the magma dike into the shallow crust. However, the assumption is useful for estimating the minimum amount

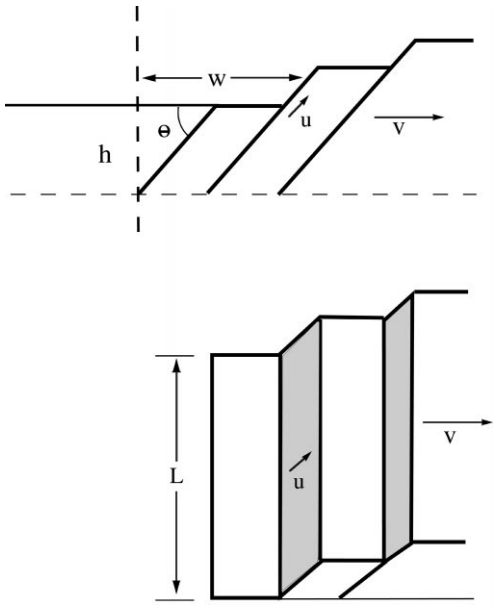

Fig. 10. Diagram of the geometry used for modeling the extension of the median valley inner floor by slip on inward-facing normal faults. v is half-spreading rate, h is depth of brittle lithosphere, w is half-width of valley inner floor, L is active segment length, θ is fault dip angle, and u is average fault slip during an earthquake. Model results based on this simplified geometry estimate that the total seismicity recorded during the 1996 northern Gorda Ridge event accounts for approximately one year of seafloor spreading, based on a full spreading rate of 5.5 cm/yr.

of ridge extension that occurred during the 1996 eruption based on the hydrophone recorded earthquakes alone.

Assume a segment of median valley floor (Fig. 10) with a half-width w, an along axis segment length of L, a thickness h of the brittle layer, and that all extension of this layer occurs by seismogenic normal faulting on planar faults extending to depth h and dipping on an inward angle θ. Following the formulation of Solomon et al. (1988), during a time interval t (which includes the earthquake swarm within the median valley), the inner floor has widened. The accumulated seismic moment release per unit time, including both sides of the valley, is then given by

$$\frac{M_0}{t} = \frac{2\mu L v h}{(\sin\theta\cos\theta)}, \tag{2}$$

where $\mu = 3 \times 10^{11}$ dyne cm^{-2} is the shear modulus of oceanic crust. Note that Eq. (2) is independent of the width of the valley inner floor and fault slip during an earthquake, both of which are proportional to horizontal strain and can be factored out of the equation. The length of the active Gorda Ridge segment is assumed to coincide with the T-wave epicenter distribution (~ 40 km). The thickness h of the

elastic crust is constrained by the hypocenters of the Gorda swarm seismically recorded earthquakes to be 9 ± 3 km, and the mean fault dips θ are constrained from centroid-moment tensor solutions to be $\sim 50^{\circ}$ (J. Braunmiller, pers. comm.). Solving Eq. (2) for half-spreading rate v suggests that the 1996 Gorda Ridge episode resulted in 2.96 cm of half-, or 5.92 cm of full-horizontal extension across the median valley during the ~ 21.7-day time period of the swarm. The long-term (5 my) full-spreading rate of the Gorda Ridge estimated from magnetic lineations is 5.5 cm/yr (Wilson, 1993), implying the February–March 1996 T-wave swarm accounted for approximately one year of seafloor spreading along the northern Gorda Ridge segment. This estimate clearly does not reflect a reasonable recurrance interval for magmatic events since (1) the actual seismic moment release may be far greater than estimated for the reasons stated above; (2) the northern Gorda Ridge segment is subject to continuous seismic activity apart from magma injection episodes; and (3) over seven years of continuous monitoring from SOSUS has detected only the 1996 event along the northern Gorda Ridge. This estimate of ridge-crest extension from seismic moment release, although limited, does provide a basis for comparison with other seafloor spreading episodes.

6. Summary

(1) The hydroacoustic monitoring technique was again successful in detecting and locating volcanic activity on the seafloor. In this case, only an incomplete acoustic record was available due to listening-array downtime, but field parties were still directed to the correct location on the northern Gorda Ridge;

(2) As was the case with the 1993 eruptive event on the CoAxial segment of the Juan de Fuca Ridge, the seismicity was detected for approximately three weeks, providing adequate time for a field response effort in spite of difficult weather conditions;

(3) Unlike the simple lateral dike injection followed by eruption inferred at CoAxial segment, the Gorda Ridge event involved multiple down-rift migrations of seismicity, interpreted to represent multiple magma intrusions and possibly multiple eruptive events. It is likely that these multiple magma pulses occurred along the path of the initial injection and represent renewed pressure in the magma system and extension or widening of the dike;

(4) T-wave rise times indicate shoaling of the dike and possibly eruption. The overall duration of the rise times was consistently longer than observed at CoAxial segment. Factors involved might include different crustal properties or rougher seafloor terrain on the Gorda Ridge;

(5) Seismic, and presumably dike, propagation rates for the Gorda Ridge event were approximately 0.55 m/s, which is twice the rate observed during the CoAxial segment episode. If significant, this increased propagation rate may reflect the higher relief of the Gorda Ridge segment and/or the nature of the crust being intruded;

(6) Detailed comparison of the hydroacoustic interpretation with various field observations offers a consistent if incomplete story. There is an apparent offset

between the epicenter locations and the location of both event plumes and seafloor lava flows;

(7) Estimation of total seismic moment release derived from hydroacoustic T-waves indicates a minimum estimated extension for the event of 5.9 cm. Although this figure almost certainly represents an underestimate, it is a valuable technique for comparing other seafloor spreading episodes.

Hydroacoustic real-time monitoring of the northeast Pacific spreading centers represents the best method of detecting active seafloor spreading episodes over large areas and in real time. This monitoring effort continues to direct field parties to the sites of active seafloor spreading and provide insights into the nature of oceanic crustal accretion processes. Current plans call for the continuous monitoring of the northeast Pacific Ocean spreading centers into the foreseeable future.

Acknowledgements

Thanks to the personnel at U.S. Naval Ocean Processing Facility, Whidbey Island, Washington, for their continued support of this environmental monitoring effort. Thanks also to the NOAA fleet, especially the NOAA ships *McArthur* and *Discoverer*, and NSF and the UNOLS vessel *Wecoma* for altering their schedules to allow a rapid response. Reviews from Kristin Rohr, an anonymous reviewer, and Bill Chadwick greatly improved the manuscript. Special thanks for the faith shown by our many colleagues who braved the North Pacific winter seas to study the event. This project is funded by the NOAA VENTS Program. PMEL Contribution #1870.

References

Baker, E.T., 1998. Patterns of event and chronic plume venting following a magmatic intrusion: new perspectives from the 1996 Gorda Ridge eruption. Deep-Sea Research II 45, 2599–2618.

Baker, E.T., Massoth, G.J., Feely, R.A., Embley, R.W., Thomson, R.E. Burd, B.J., 1995, Hydrothermal event plumes from the CoAxial seafloor eruption site, Juan de Fuca Ridge. Geophysical Research Letters 22(2), 147–150.

Chadwick Jr, W.W., Embley, R.W., Shank, T.M., 1998. The 1996 Gorda Ridge eruption: geologic mapping, sidescan sonar, and SeaBeam comparison results. Deep-Sea Research II 45, 2547–2569.

Chadwick Jr, W.W., Embley, R.W., Fox, C.G., 1995. SeaBeam depth changes associated with recent lava flows, CoAxial segment eruption, Juan de Fuca Ridge: evidence for multiple eruptions between 1981–1993, Geophysical Research Letters 22(2), 167–170.

Cowen, J.P., Bertram, M.A., Baker, E.T., Feely, R.A., Summit, M., 1998. Geomicrobial transformation of manganese in Gorda Ridge event plumes. Deep-Sea Research II 45, 2713–2737.

Dziak, R.P., Fox, C.G., Slack, P.D., 1996. T-wave source level and earthquake fault parameters: Empirically derived scaling relationships. Journal of the Acoustical Society of America 100(4), 2639.

Dziak, R.P., Fox, C.G., Matsumoto, H., Schreiner, A.E., 1997. The April 1992 Cape Mendocino earthquake sequence: seismo-acoustic analysis utilizing fixed hydrophone arrays. Marine Geophysical Researches 19(2), 136–162.

Dziak, R.P., Fox, C.G., Schreiner, A.E., 1995. The June–July 1993 seismo-acoustic event at CoAxial segment, Juan de Fuca Ridge: evidence for lateral dike injection. Geophysical Research Letters 22(2), 135–138.

Embley, R.W., Chadwick Jr, W.W., Jonasson, I.A., Butterfield, D.A., Baker, R.T., 1995. Spectra and magnitudes of T-waves from the 1993 earthquake swarm on the Juan de Fuca Ridge. Geophysical Research Letters 22(2), 139–142.

Feely, R.A., Baker, E.T., Lebon, G.T., Gendron, J.F., Massoth, G.J., Mordy, C.W., 1998. Chemical variations of hydrothermal particles in the 1996 Gorda Ridge Event and chronic plumes. Deep-Sea Research II 45, 2637–2664.

Fox, C.G., 1995. Special collection on the June 1993 volcanic eruption on the CoAxial segment, Juan de Fuca Ridge. Geophysical Research Letters 22(2), 129–130.

Fox, C.G., Radford, W.E., Dziak, R.P., Lau, T.-K., Matsumoto, H., Schreiner, A.E., 1995. Acoustic detection of a seafloor spreading episode on the Juan de Fuca Ridge using military hydrophone arrays. Geophysical Research Letters 22(2), 131–134.

Fox, C.G., Dziak, R.P., Marumoto, H., Schreiner, A.E., 1994. Potential for monitoring low-level seismicity on the Juan de Fuca Ridge using military hydrophone arrays. Marine Technology Society Journal 27(4), 22–30.

Fox, Christopher G., William W. Chadwick, Robert W. Embley, 1992. Detection of changes in ridge crest morphology using repeated multibeam sonar surveys. Journal of Geophysical Research 97(B7), 11 149–11 162.

Hooft, E.E.E., Detrick, R.S., 1995. Relationship between axial morphology, crustal thickness, and mantle temperatures along the Juan de Fuca and Gorda Ridges. Journal of Geophysical Research 100(B11), 22 499–22 508.

Lupton, J.E., Baker, E.T., Massoth, G.J., Thomson, R.E., Burd, B.J., Butterfield, D.A., Embley, R.W., Cannon, G.A., 1995. Variations in water-column ^{3}He/heat ratios associated with the 1993 CoAxial event, Juan de Fuca Ridge, Geophysical Research Letters 22(2), 155–158.

Massoth, G.J., Baker, E.T., Feely, R.A., Lupton, J.E., Collier, R.W., Gendron, J.F., Roe, K.K., Maenner, S.M., Resing, J.A., 1998. Manganese and iron in hydrothermal plumes resulting from the 1996 Gorda Ridge Event. Deep-Sea Research II 45, 2683–2712.

Massoth, G.J., Baker, E.T., Feely, R.A., Butterfield, D.A., Embley, R.E., Lupton, J.E., Thomson, R.E., Cannon, G.A., 1995. Observations of manganese and iron at the CoAxial seafloor eruption site, Juan de Fuca Ridge, Geophysical Research Letters 22(2), 151–154.

Schreiner, A.E., Fox, C.G., Dziak, R.P., 1995. Spectra and magnitudes of T-waves from the 1993 earthquake swarm on the Juan de Fuca Ridge. Geophysical Research Letters 22(2), 139–142.

Solomon, S.C., Huang, P.Y., Menke, L., 1988. The seismic moment budget of slowly spreading ridges. Nature 334, 58–60.

Wilson, D.S., 1993. Confidence intervals for motion and deformation of the Juan de Fuca plate. Journal of Geophysical Research 98, 16 053–16 071.